

Relaxor behavior of pulsed laser deposited ferroelectric ($\text{Pb}_{1-x}\text{La}_x$)($\text{Zr}_{0.65}\text{Ti}_{0.35}$) O_3 films

M. Tyunina, J. Levoska, A. Sternberg, and S. Leppävuori

Citation: [Journal of Applied Physics](#) **84**, 6800 (1998); doi: 10.1063/1.369012

View online: <http://dx.doi.org/10.1063/1.369012>

View Table of Contents: <http://scitation.aip.org/content/aip/journal/jap/84/12?ver=pdfcov>

Published by the [AIP Publishing](#)

Articles you may be interested in

[Effects of postdeposition annealing on the dielectric properties of antiferroelectric lanthanum-doped lead zirconate stannate titanate thin films derived from pulsed laser deposition](#)

[J. Appl. Phys.](#) **96**, 5830 (2004); 10.1063/1.1804226

[Dielectric properties of lead lanthanum zirconate stannate titanate antiferroelectric thin films prepared by pulsed laser deposition](#)

[J. Appl. Phys.](#) **95**, 6341 (2004); 10.1063/1.1715136

[Ferroelectric silver niobate-tantalate thin films](#)

[Appl. Phys. Lett.](#) **77**, 4416 (2000); 10.1063/1.1334655

[Field-induced dielectric properties of laser ablated antiferroelectric \(\$\text{Pb}_{0.99}\text{Nb}_{0.02}\$ \)\(\$\text{Zr}_{0.57}\text{Sn}_{0.38}\text{Ti}_{0.05}\$ \) \$\text{O}_3\$ thin films](#)

[Appl. Phys. Lett.](#) **77**, 4208 (2000); 10.1063/1.1332977

[Dielectric properties of pulsed laser deposited films of \$\text{PbMg}_{1/3}\text{Nb}_{2/3}\$ - \$\text{PbTiO}_3\$ and \$\text{PbSc}_{1/2}\text{Nb}_{1/2}\text{O}_3\$ - \$\text{PbTiO}_3\$ relaxor ferroelectrics](#)

[J. Appl. Phys.](#) **86**, 5179 (1999); 10.1063/1.371497



Launching in 2016!

The future of applied photonics research is here

OPEN
ACCESS

AIP | APL
Photonics

Relaxor behavior of pulsed laser deposited ferroelectric $(\text{Pb}_{1-x}\text{La}_x)(\text{Zr}_{0.65}\text{Ti}_{0.35})\text{O}_3$ films

M. Tyunina

*Institute of Solid State Physics, University of Latvia, 8 Kengaraga, Riga LV-1063, Latvia and
Microelectronics Laboratory and EMPART Research Group of Infotech Oulu, University of Oulu,
FIN-90571 Oulu, Finland*

J. Levoska^{a)}

*Microelectronics Laboratory and EMPART Research Group of Infotech Oulu, University of Oulu,
FIN-90571 Oulu, Finland*

A. Sternberg

Institute of Solid State Physics, University of Latvia, 8 Kengaraga, Riga LV-1063, Latvia

S. Leppävuori

*Microelectronics Laboratory and EMPART Research Group of Infotech Oulu, University of Oulu,
FIN-90571 Oulu, Finland*

(Received 15 June 1998; accepted for publication 16 September 1998)

The dielectric behavior of pulsed laser deposited ferroelectric $(\text{Pb}_{1-x}\text{La}_x)(\text{Zr}_{0.65}\text{Ti}_{0.35})\text{O}_3$ films (PLZT $x/65/35$, $x=0-9.75$ at. %) has been studied experimentally. Epitaxial stoichiometric PLZT films were formed on a pulsed laser deposited layer of $\text{La}_{0.5}\text{Sr}_{0.5}\text{CoO}_3$ (LSCO) on MgO (100) single-crystal substrates. The dielectric permittivity and loss tangent of the resulting heterostructures were measured in the temperature range of 20–350 °C at a frequency of 100 Hz–1 MHz. A peak around 130–350 °C was observed in the dielectric permittivity versus temperature curves. The peak exhibited a relaxor type behavior. Its position was a nonmonotonic function of the La content and depended on the microstructure of the film. The broadening of the peak of the dielectric permittivity was larger than that in the ceramic PLZT and it also depended on the La content and microstructure of the film. The broadening depended on the temperature and frequency ranges: master curves of the normalized dielectric permittivity versus normalized temperature were obtained for PLZT films. The results are discussed in terms of the random field theory for relaxor ferroelectrics and the models for finite-size ferroelectrics. © 1998 American Institute of Physics. [S0021-8979(98)05224-4]

I. INTRODUCTION

La-modified lead zirconate titanate $(\text{Pb}_{1-x}\text{La}_x)(\text{Zr}_{0.65}\text{Ti}_{0.35})\text{O}_3$, or PLZT $x/65/35$, with the La content $x=4-14$ at. %, belongs to the family of perovskite relaxor ferroelectrics. In contrast to ordinary ferroelectrics, relaxors exhibit anomalies in their dielectric, polarization, electromechanical, optical, and electrooptical properties within a broad temperature region about a temperature T_m , corresponding to the maximum in the dielectric permittivity. The phase transition is referred to as the “diffuse phase transition” (DPT). Due to the anomalies in the properties, in particular, high values of dielectric permittivity and very large electromechanical and electrooptic coefficients, relaxors find a variety of applications in capacitors, actuators, optoelectronic modulators, etc., and attract much interest.^{1,2}

Great efforts have been made to gain an understanding the origin of such anomalies in the relaxor properties. Many important models were proposed for the DPT.³ In the pioneering works,^{4,5} the DPT was related to chemical heterogeneities with a consequent smearing of the local Curie temperatures. Later, the relaxor system was considered as a

dipole glass with local regions of long-range order.⁶ A decade ago a superparaelectric model⁷ was proposed, with the DPT generated by mesoscopic heterogeneities. The existence of nanometric polar clusters and random interactions among them result in a spin-glass-like state with the broadening of the Curie region.⁸ In another model⁹ the relaxors were formally compared with magnetic spin glasses. The dielectric properties of the relaxors are controlled by a broad spectrum of relaxation times.¹⁰ This was considered as resulting from the size distribution of the polar regions,¹¹ from the distribution of local transition temperatures,¹² from the temperature dependence of the reorientation frequency of polar clusters,¹³ or from the thermally activated flips of the polar regions.¹⁴ An approach within the random field theory was recently developed.^{15,16} The relaxors were considered as systems with random sites and orientations of electric dipoles, lattice vacancies and other defects and impurities embedded into the paraelectric “host” lattice. The random fields, created by the underlying disorder, were shown to be responsible for the shift of the transition temperature. Despite the qualitative agreement between the models and experimental data^{17–20} the detailed physical process of the DPT is still not completely clear.

^{a)} Author to whom correspondence should be addressed; electronic mail: jlev@ee.oulu.fi

It should be noted that the above-mentioned studies were related mainly to ferroelectric ceramics and single crystals. However, in recent years much attention has been paid to ferroelectric thin films.²¹ The interest derives from the promising applications of these films, such as a new generation of nonvolatile memories and microelectromechanical systems. The thin film form of the material possesses specific properties. It was demonstrated^{22–25} that in finite-size ferroelectrics, including thin films and superlattices, the Curie temperature, dielectric permittivity, polarization, and coercive field can be drastically altered with respect to the sample size (film thickness) and surface preparation. A size driven phase transition from the ferroelectric to paraelectric state in thin films could be accompanied by a dielectric divergence. The behavior bears a resemblance to the relaxor ferroelectric transition. In this respect, the detailed experimental studies of the phase transition in relaxor ferroelectric thin films can be of fundamental importance.

The present work was focused on the experimental study of the dielectric properties of pulsed laser deposited PLZT 0–9.75/65/35 thin films. The studies of PLZT x /65/35 for a large x range embrace materials with different levels of compositional order (or heterogeneity), which is important for clarifying the nature of the DPT. On the other hand, pulsed laser deposition enables the production of epitaxial and highly oriented films with variable domain configurations and microstructures.²⁶ This makes it possible to investigate systems of a similar composition but of a different level of order (heterogeneity).

The dielectric permittivity and loss tangent of PLZT films, produced by laser ablation on LSCO/MgO substrates, were measured in the temperature range of 20–350 °C and in the frequency range of 100 Hz–1 MHz. The results of our experimental study showed that the dielectric properties and the phase transition in PLZT films are strongly influenced by the La content and microstructure in the films, as well as by the interfaces in the thin film heterostructures.

II. EXPERIMENT

The films were produced by laser ablation using an XeCl excimer laser. To reduce droplet formation and film surface roughening, the target rotation was combined with a two-dimensional scanning of the laser radiation over the target surface. The substrate was placed opposite and parallel to the target (on-axis deposition). The fluence of the incident laser radiation on the target surface was maintained at 3 J/cm².

The composition and microstructure of the films were controlled by the variation of the deposition conditions. The pressure of ambient oxygen was varied in the range of 0.2–1.0 mbar. The size of the laser spot on the target surface was changed from 0.6 to 6.0 mm². This was accompanied by changes in the target-to-substrate distance from 30 to 50 mm.

The PLZT films were deposited using dense ceramic targets of PLZT x /65/35 with the La content x = 0–9.75 at. % sintered at the ISSP, University of Latvia. The temperature of PLZT deposition was 600 °C. PLZT films were formed on the top of La_{0.5}Sr_{0.5}CoO₃ (LSCO) layers, produced by *in situ*

pulsed laser deposition (for the details, see Ref. 27) on MgO (100) single-crystal substrates.

To compare accurately the properties of the films, the thickness of the films was kept constant and equal to 250 nm for PLZT films and 100 nm for LSCO films. This was achieved by adjusting the duration of deposition with respect to deposition conditions and, correspondingly, to the growth rate.²⁸

The elemental composition and thickness of the films were analyzed by energy dispersive x-ray spectroscopy (EDX) using a scanning electron microscope (SEM). The obtained spectra were processed with STRATA 5.0 software.

The morphology of the film surface was examined by field emission scanning electron microscopy (FESEM) and atomic force microscopy (AFM). X-ray diffraction studies of the crystal structure and orientation of the films were performed by both θ – 2θ diffraction patterns and ϕ scans on a texture goniometer, employing Cu $K\alpha$ radiation.

The electrical characterisation of the heterostructures was performed using a probe station. For this, Pt contact pads were pulsed laser deposited on the top of the PLZT film and on the top of the part of LSCO layer which was masked during the PLZT deposition.

The dielectric properties of the PLZT films were evaluated by the “zero-field” measurement of capacitance and loss tangent of the corresponding heterostructures. The measurements were carried out using an HP4284 LCR meter over the frequency range of 100 Hz–1 MHz. The dielectric permittivity was calculated from the measured capacitance using the geometric parameters of the heterostructures in the parallel-plate capacitance model. The temperature of the samples was varied in the range of 20–350 °C by heating and cooling continuously at a rate of 0.5 °C/min. The temperature controller and LCR meter were interfaced to a computer. Ferroelectric properties of PLZT films were evaluated by room temperature measurements of polarization of the heterostructures using a modified Sawyer–Tower circuit.

III. RESULTS

A. Composition and microstructure of PLZT films

The parameters of the deposition process were optimized experimentally to obtain films of proper stoichiometry. In particular, the EDX measurements showed that the film composition was very sensitive to changes in the ambient oxygen pressure from vacuum to approximately 0.2 mbar, while a further increase in oxygen pressure resulted in stoichiometric films. This is illustrated in Fig. 1, where the measured ratios of the atomic content of Pb to the content of Ti and of Pb to Zr are plotted as a function of oxygen pressure.

Increasing the size of the laser focal spot without changing the fluence of the incident radiation led to an increase of both the amount of ablated material per pulse and of the energy of ablated species. The corresponding change of the film composition was corrected by an increase in the target-to-substrate distance and a consequent increase in the number of collisions of ablated species with ambient gas molecules which decreases the energy of the species.

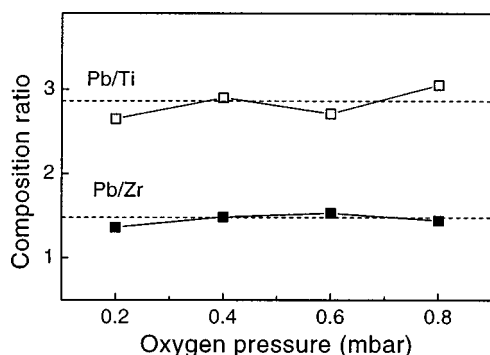


FIG. 1. Elemental composition of a PLZT film as a function of oxygen pressure. The ratio of the atomic content of Pb to the atomic content of Zr and of Pb to Ti were measured by EDX in the films deposited at 600 °C.

Stoichiometric PLZT 0–9.75/65/35 films were obtained using two sets of process parameters: (1) the laser focal spot 0.6 mm², target-to-substrate distance 30 mm and oxygen pressure 0.8 mbar (first series of films); (2) the laser focal spot 6.0 mm², target-to-substrate distance 50 mm, oxygen pressure 0.8 and 0.5 mbar (second series of films).

The stoichiometric PLZT films deposited under optimum conditions were pure perovskite and highly oriented with (00 l) type planes parallel to the substrate surface [Fig. 2(a)]. The relative volume of the (110)-oriented phase, evaluated using the integrated intensity of the corresponding peaks in θ – 2θ x-ray diffraction patterns, did not exceed 0.5%. The

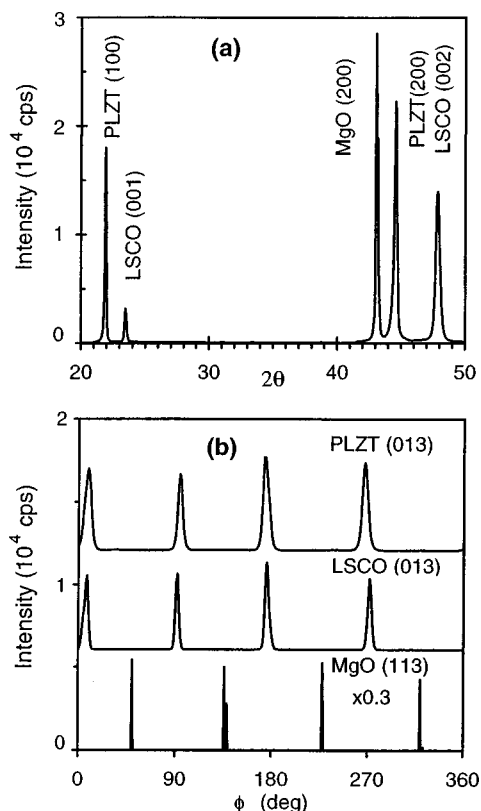


FIG. 2. (a) A typical θ – 2θ x-ray diffraction pattern of a PLZT/LSCO/MgO heterostructure (PLZT 4.5/65/35). (b) A ϕ scan through the indicated reciprocal lattice points of a PLZT 9.75/65/35 heterostructure showing the in-plane epitaxial relationship PLZT[100]||LSCO[100]||MgO[100].

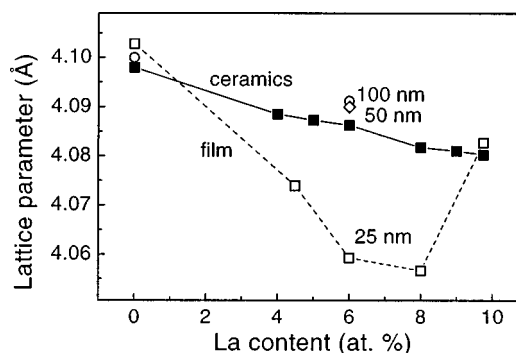


FIG. 3. Lattice parameter of PLZT films as a function of the La content and deposition conditions. PLZT films were deposited using a small focal spot and 0.8 mbar oxygen (open squares, grain size about 25 nm), a large focal spot and 0.5 mbar oxygen (open circles, grain size about 100 nm), or 0.8 mbar oxygen (open diamond, grain size about 50 nm). The lattice parameter of PLZT bulk ceramics is shown for comparison (solid squares).

in-plane epitaxy of the films was confirmed by ϕ scans, which showed an orientation relationship of trigonal PLZT [001] parallel with pseudocubic LSCO [001] and MgO [001] [Fig. 2(b)].

The lattice parameter of the PLZT films was calculated from the positions of the peaks in the θ – 2θ x-ray diffraction patterns, giving the parameter a in the direction perpendicular to the substrate surface. The corrections were made with reference to the position of the MgO (200) reflection and LSCO peaks. The obtained values are plotted in Fig. 3 with respect to the La content and deposition conditions.

In ferroelectric PLZT x /65/35 with trigonal symmetry, the increase in the La content from 0 to 8 at. % is known to result in a decrease in the lattice parameter and an increase in the trigonal angle. The transformation to cubic symmetry takes place for $x > 8$ at. %. The lattice parameter a in the films of the first series (deposited using a small laser spot) decreased with the La doping and was generally smaller than in bulk ceramics (Fig. 3). However, a increased up to the bulk value with 9.75 at. % La. This increase might be connected with the formation of the cubic phase, which had more favorable conditions of growth on the cubic substrate compared with the formation of the trigonal phase. The lattice parameter in the films of the second series (deposited using the larger laser spot) was close to the bulk value.

The observed dependence of the lattice parameter on the deposition conditions and the La content in the film was accompanied by considerable changes in the surface morphology. Depositions using the small laser spot resulted in films with a rather small grain size. The increase in the laser spot resulted in the formation of much larger grains. In Fig. 4, FESEM images of some of the films are presented. The surface of a PLZT 0/65/35 film of the first series, deposited using the small spot and 0.8 mbar oxygen [Fig. 4(a)], contained nearly “square” oriented grains of 10–50 nm in lateral dimensions. A PLZT 0/65/35 film of the second series (large spot, 0.5 mbar oxygen) consisted of “square” oriented grains with sharp edges [Fig. 4(b)]. The maximum size of the grains reached 200 nm. Smaller grains were detected between larger ones.

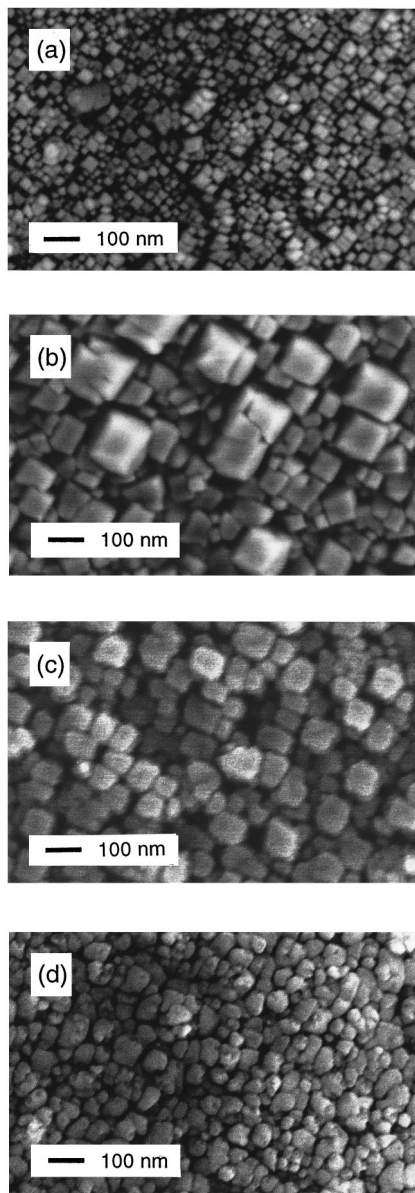


FIG. 4. FESEM images of the surface of PLZT films: (a) a PLZT 0/65/35 film of the first series, (b) a PLZT 0/65/35 film of the second series, (c) a PLZT 6/65/35 film of the second series, (d) a PLZT 6/65/35 film of the second series. The films were deposited using the smaller focal spot and 0.8 mbar oxygen (a), using the larger focal spot and 0.5 mbar oxygen (b), (c), using the larger focal spot and 0.8 mbar oxygen.

The morphology of the films depended on the La doping. Figure 4(c) shows a FESEM image of a PLZT 6/65/35 film deposited under the same conditions as PLZT 6/65/35 in Fig. 4(b). The La doping to 6 at. % resulted in less sharp, slightly rounded edges of the “square” oriented grains of 50–150 nm in diameter. The tendency for the grains to become smaller and more round shaped with increased La doping was well expressed in the samples of the second series. The corresponding changes in the films of the first series were not detected, perhaps due to the generally rather small grain size.

The variation in the oxygen pressure also had an effect on the morphology. A PLZT 6/65/35 film deposited using the larger spot and 0.8 mbar oxygen [Fig. 4(d)] contained

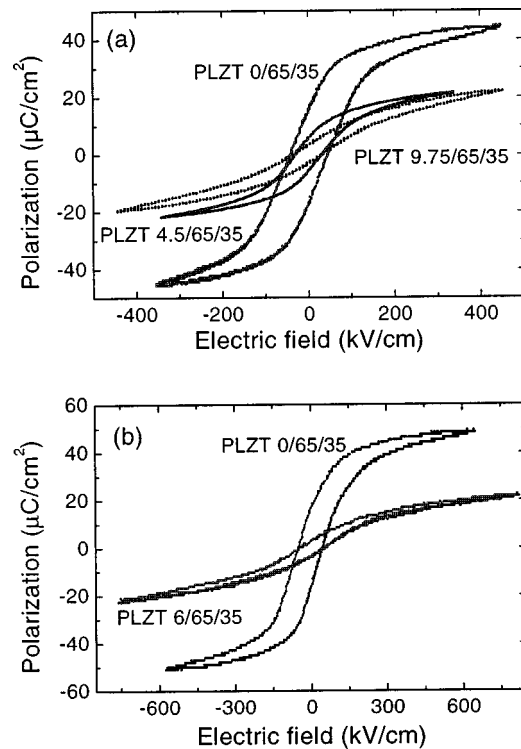


FIG. 5. Polarization-electric field hysteresis loops of PLZT films (a) of the first series with small grain size and (b) of the second series with larger grains, measured at 15 Hz. The thickness of the PLZT films was 250 nm.

round shaped grains of 20–100 nm in diameter. The shape, size, and orientation of the grains differed from those in the PLZT 6/65/35 film deposited using a lower oxygen pressure [Fig. 4(c)].

The observed dependence of the microstructure of the films on the deposition conditions could be analyzed on the basis of the generally accepted model of epitaxial growth. But this was not the purpose of the present work. The important result was that, whatever the underlying mechanism, oriented films of proper stoichiometry, but with different microstructure, were obtained. In particular, in the PLZT 6/65/35 films the lattice parameter varied in the range of 4.057–4.086 Å and the average grain size was 25–100 nm (Fig. 3).

B. Ferroelectric hysteresis

All deposited heterostructures demonstrated hysteresis of polarization. The polarization-electric field (P - E) hysteresis loops measured at room temperature at 15 Hz are presented in Fig. 5. It can be seen that, with an increase in the La content from 0 to 9.75 at. % in the films of the first series, with the grain size about 25 nm, the remnant polarization decreased from approximately 17 to 5 $\mu\text{C}/\text{cm}^2$ and the coercive field from 50 to 35 kV/cm. A similar tendency was observed in the films of the second series, with the larger grains [Fig. 5(b)]. No significant differences in P - E loops were detected with respect to the deposition conditions, except a minor enhancement of polarization in PLZT 0/65/35 films of the second series.

The polarization behavior in the films was consistent with the observations by other authors.²⁹ The lower values of polarization in the films compared to those in the bulk ceramics could be explained by the suppression of polarization at the interfaces. The effect was theoretically studied using different approaches. Both the description of the system by a Ginzburg–Landau functional with space-dependent coefficients²² and the analysis based on the phenomenological free energy²³ have demonstrated the thickness dependence of the polarization in ferroelectric thin films.

The dependence of the ferroelectric hysteresis on the La doping was in agreement with the bulk ceramic PLZT and experimental data on PLZT films. However, the influence of the film microstructure on the P - E loops was insignificant. This could be connected with the dominant effect of the interfaces on the resultant polarization in the heterostructure.

C. Dielectric permittivity and loss tangent

The dielectric permittivity, ϵ , and loss tangent, $\tan \delta$, of the heterostructures were studied as a function of the temperature T and the measurement frequency f . Some results are presented in Figs. 6 and 7, where the dielectric permittivity and loss tangent measured during cooling are plotted versus the measurement temperature for different measurement frequencies. The basic features were the following.

The room temperature values of ϵ lay in the range 250–400. They were lower than in the bulk ceramics, but in agreement with other experimental data³⁰ and theoretical evaluations.^{23,24,31,32}

All deposited PLZT films, irrespective of the composition and microstructure, demonstrated an increase in ϵ located around 340 °C. Along with this, broad peaks in dielectric permittivity located in the lower temperature region were observed in the films with the La content of 4.5–9.75 at. %. The position of these peaks shifted to higher temperatures with increasing frequency, while the magnitude of the peaks decreased.

The room temperature value of $\tan \delta$ in the heterostructures increased from 0.01–0.03 to 0.5–1.0 with an increase in the measurement frequency from 100 Hz to 1 MHz. In PLZT 4.5–9.75/65/35 films, as with the temperature dependence of ϵ , the $\tan \delta$ curves demonstrated an increase around a higher temperature of 340 °C and a peak around a lower temperature. The magnitude of the peak increased with the frequency. The peak of $\tan \delta$ in PLZT films tended to shift towards higher temperatures with the increase in the measurement frequency. This was accompanied by an increase in its magnitude.

The observed increase in ϵ at higher temperatures could be expected from the analysis²⁵ of thin ferroelectric films in the frame of the Ising model. The existence of two peaks in the dielectric susceptibility–temperature curves was predicted²⁵ from the modification of the exchange constant and the transverse field in the surface (interface) layer. The position of one peak was expected around the bulk Curie point, while another peak could be shifted to a higher temperature. In the present work, however, the studies of the high temperature increase in ϵ were restricted by the increase

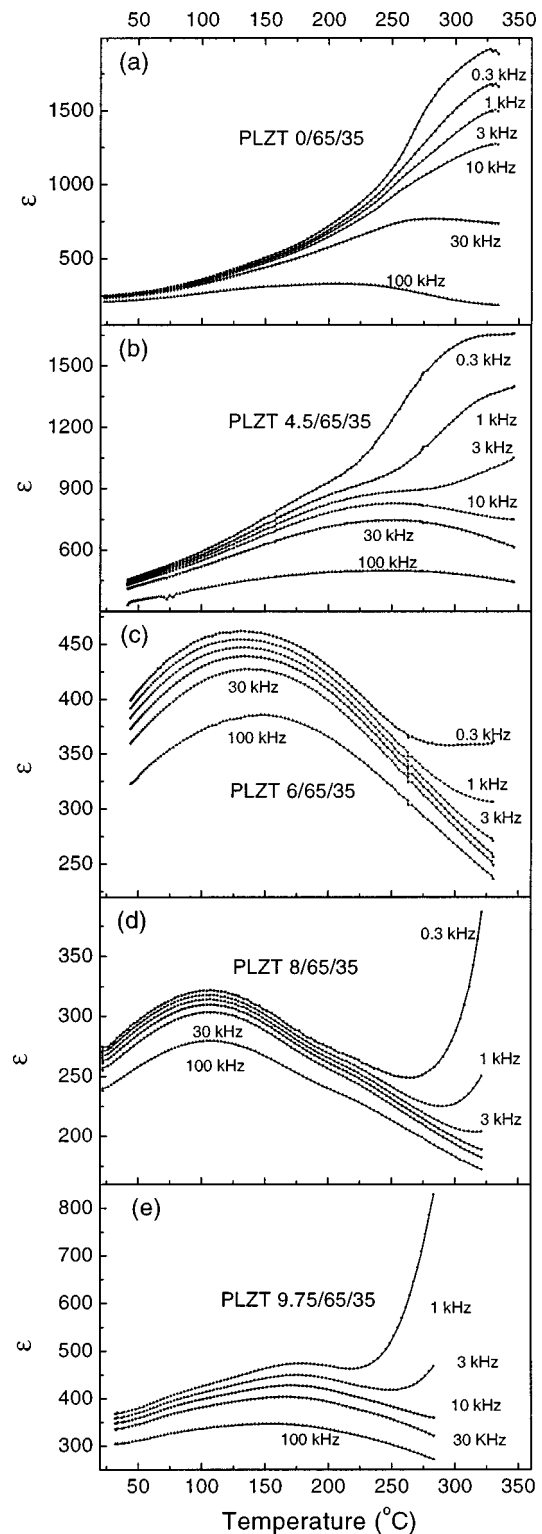


FIG. 6. Dielectric permittivity ϵ as a function of temperature measured at different frequencies with a cooling rate of 0.5 °C/min in PLZT $x/65/35$ films: (a) $x=0$, (b) 4.5 at. %, (c) 6 at. %, (d) 8 at. %, (e) 9.75 at. %.

in loss tangent and possible changes in the Pt-film interfaces at the higher temperatures. Only the lower temperature peaks in ϵ and $\tan \delta$ were taken into consideration.

The position and behavior of the peaks of ϵ and $\tan \delta$ very closely resembled typical relaxor ferroelectric behavior. To make more definite conclusions about the origin of the

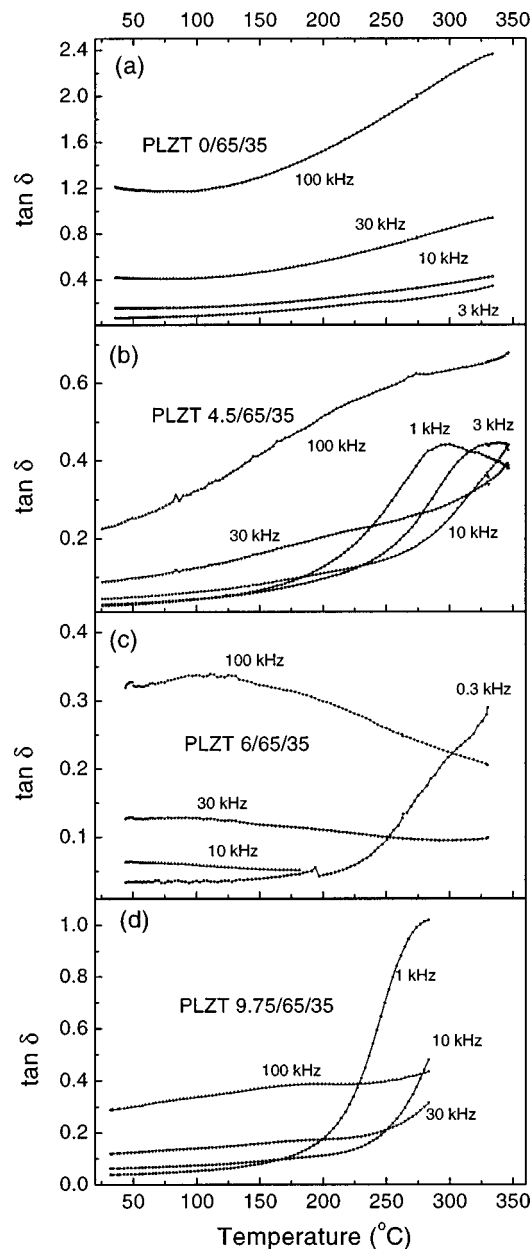


FIG. 7. Loss tangent $\tan \delta$ as a function of temperature measured at different frequencies with a cooling rate of $0.5^\circ\text{C}/\text{min}$ in PLZT $x/65/35$ films: (a) $x=0$, (b) 4.5 at. %, (c) 6 at. %, (d) 9.75 at. %.

dielectric properties in the PLZT films, the exact position and width of the observed peaks were determined and analyzed.

D. Temperature of transition

It can be seen, from Fig. 6, that both an increase at higher temperature and lower temperature peaks in dielectric permittivity were broad and overlapping. This made it rather difficult to determine the exact positions of the peaks and their width. The peaks were separated using a peak fitting software assuming symmetric peaks with respect to the position of the maxima. In part, this assumption was based on the analysis of the shape of the dielectric permittivity–temperature curves measured at high frequencies in PLZT 6/65/35 and PLZT 8/65/35 films [Figs. 6(c), 6(d)]. The mag-

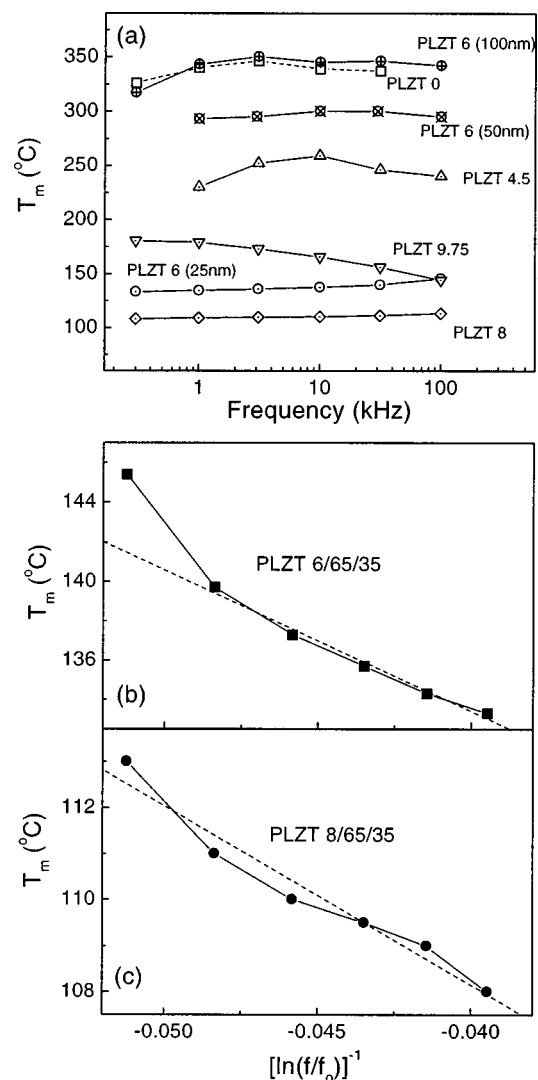


FIG. 8. Positions T_m of the peaks in the dielectric permittivity ϵ determined at different measurement frequencies in PLZT $x/65/35$ films with the grain size about 25 nm (no special marks at the curves) and in PLZT 6/65/35 films with the grain size about 100 and about 50 nm (marked in brackets). Fits to the Vogel–Fulcher relationship are shown by dashed lines (b), (c).

nitude of the increase at higher temperature was insignificant at high frequencies. The shape of the lower temperature peaks appeared to be symmetric under these conditions.

The peak fitting was carried out for the dielectric permittivity–temperature and loss tangent–temperature curves. The temperatures of the maxima, determined by the fitting, are presented in Figs. 8 and 9 with respect to the measurement frequency and film composition.

The position T_m of the peak of dielectric permittivity in PLZT 0/65/35 films was found to be around $325\text{--}340^\circ\text{C}$ in a broad frequency range [Fig. 8(a)]. The measured value of $T_m = 325\text{--}340^\circ\text{C}$ was in a good agreement with the Curie point in the ceramic PZT 0/65/35.

The position of T_m in PLZT films of the first series (films with small grain size) was a function of the La content. T_m decreased from approximately 250 to 110°C with an increase in the La content from 4.5 to 8 at. %. The position of T_m in the PLZT 9.75/65/35 films, however, was around 160°C .

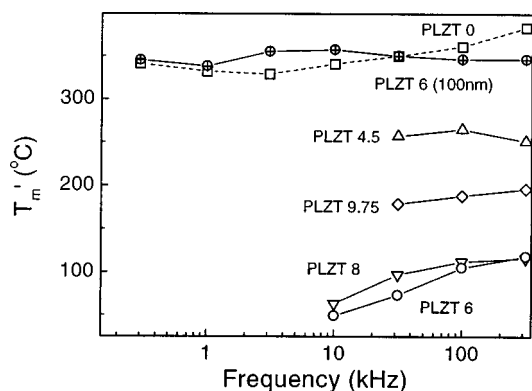


FIG. 9. Position T'_m of the peak in loss tangent $\tan \delta$ determined at different measurement frequencies in PLZT $x/65/35$ films with the grain size about 25 nm (no special marks at the curves) and in PLZT 6/65/35 film with the grain size about 100 nm (marked in brackets).

The temperature T_m depended also on the deposition conditions of the films. In particular, PLZT 6/65/35 films of the second series (films with larger grains) demonstrated a considerably higher T_m compared to that in the films of the first series.

The shift of T_m towards higher temperatures with increasing frequency was well expressed in PLZT films with 6 and 8 at. % of La. In the rest of the films, this was distorted by the rather high magnitude of the increase at higher temperatures. The frequency dependence of the temperature of the dielectric peak in relaxor ferroelectrics is known to obey the empirical Vögel–Fulcher relationship (see, e.g., the discussion in Ref. 19). The temperature T_m in PLZT 6/65/35 and PLZT 8/65/35 films was found to be an approximately linear function of $[\ln(f/f_0)]^{-1}$, where f is the measurement frequency and f_0 is a constant [Figs. 8(b), 8(c)]. The fit of T_m to the Vögel–Fulcher relationship confirmed the typical relaxor type behavior in the deposited films.

The position of the peak in the loss tangent, T'_m , was a function of the La doping and also of the deposition conditions (Fig. 9). The measured values of T'_m were lower than T_m for PLZT 6–8/65/35 films. This feature, typical for relaxors, was not evident in the other films, perhaps due to the increase in $\tan \delta$ at higher temperatures.

To compare the obtained results with the properties of the bulk ceramic PLZT, the values of T_m , determined at frequencies 1–30 kHz, were plotted versus the La content (Fig. 10). The transition temperature of the ceramic PLZT $x/65/35$ was taken from the reference.³³

The tendency for the transition temperature to decrease with an increase in the La content was characteristic for the ceramic PLZT and was preserved in PLZT films as well. In contrast to the ceramics, however, PLZT films demonstrated a nonmonotonic dependence of T_m on the La doping.

An analysis of the transition temperature in the PLZT $x/65/35$ system was recently presented by Glinchuk and Farhi.¹⁵ PLZT was considered as a system with electric dipoles, La ions and different defects, embedded in the PLZT paraelectric phase and acting as sources of random electric field distribution. The phase transition temperature was then calculated. The decrease of the transition temperature was

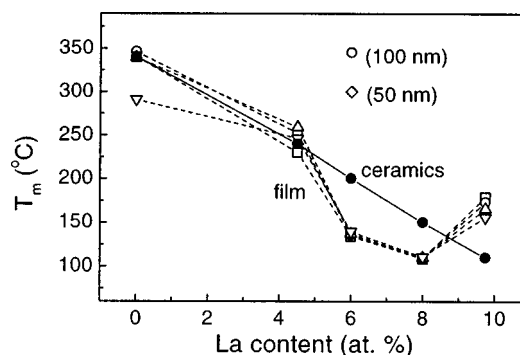


FIG. 10. Position T_m of the peak in dielectric permittivity as a function of the La content in PLZT films with the grain size about 25 nm (open symbols, no special marks at the curves) and in PLZT 6/65/35 films with the grain size of 50 nm (open diamond, marked in brackets) and with the grain size of 100 nm (open circle, marked in brackets). For comparison, the position of the dielectric peak in bulk ceramic PLZT is shown by solid circles.

shown to be a function of the concentration of the point charges and dilatation centers. It was also shown that the dependence of the transition temperature on the La content could be affected by the existence of other defects in the lattice. The defects may decrease the critical La concentration, at which the ferroelectric transition with long-range order is destroyed.

The nonmonotonic dependence of the transition temperature on the lanthanum content, observed in the present work, could be interpreted using the model¹⁵ described above. The random field distribution in PLZT films could originate from the La ions. This would result in a transition temperature in agreement with the calculations¹⁵ and with the properties of the bulk ceramic PLZT. The peculiarities of the microstructure of the laser deposited films, such as grain boundaries, misfit dislocations, residual strains, due to the epitaxial growth, etc., could act as additional sources of the random field.

To analyze this assumption, we used the data presented in Figs. 3 and 10. Both the lattice parameter and the transition temperature in the films of the first series were nonmonotonic functions of the La content and differed from the corresponding bulk values. However, although the lattice parameter of PLZT 6/65/35 films of the second series was close to the bulk value, the transition temperature was considerably higher compared to that in ceramics. The transition temperature in PLZT 6/65/35 films, including both series of the samples, correlated fairly well with the grain size in the films. The films with the larger (100 nm) grains demonstrated T_m around 350 °C. The films with smaller (50 and 25 nm) grains exhibited T_m , correspondingly, around 290 and 130 °C.

In earlier works on the finite-size ferroelectrics,³⁴ the shift in the transition temperature was ascribed to the existence of the depolarizing field at the surface of the grain or of the fine particles. However, the mechanism, proposed by Glinchuk and Farhi¹⁵ seems more suitable for the explanation of the observed correlation between T_m and the grain size in PLZT 6/65/35 films.

Assuming that the grain boundaries could contribute to the random electric field, additionally to that produced by the

La ions, it is reasonable to expect the lower transition temperature in the films with the smaller grains. Small grains and, hence, high density of the grain boundaries (or lattice defects, in fact) could reduce the critical concentration of La compared to that in a single-crystal film by a value proportional to the density of the grains (concentration of defects in Ref. 15). In other words, in films with the same La content, the transition temperature would decrease with decreasing grain size. The proposed explanation is consistent with the experimental data.

The same approach could be used to explain the reason for the nonmonotonic dependence of T_m on the La content in the films with approximately similar grain size. The growth of highly oriented PLZT $x/65/35$ films with trigonal symmetry onto cubic substrate LSCO/MgO could be accompanied by the accumulation of the unrelaxed residual strain in the film.²⁶ This could be compared with the generation of the centers of dilatation,¹⁵ resulting in a lower transition temperature. Such a growth strain would decrease with an increase in the La doping and corresponding increase in the trigonal angle. The strain should reach a minimum in films of PLZT 9.75/65/35 with a cubic symmetry. This could explain the relative increase in T_m observed in PLZT 9.75/65/35 compared to the films with a lower La content.

Thus, in PLZT $x/65/35$ films, the increase in the La content could determine both: (1) the decrease of T_m via the random field created by the La ions; and (2) the increase of T_m due to the decrease of the growth strain. These opposite tendencies could lead to a nonmonotonic dependence of T_m on the La content (Fig. 10).

In conclusion to this chapter, a peak around T_m of 130–350 °C were experimentally observed in the dielectric permittivity-temperature curves of PLZT films. The peak exhibited a relaxor type behavior. The temperature T_m was a nonmonotonic function of the lanthanum content in the film and depended on the microstructure of the film. This was explained using the random field model for the transition temperature in the PLZT $x/65/35$ system.¹⁵

E. Broadening of the phase transition

One of the main features of the phase transition in relaxor ferroelectrics is the broadening of the transition. In the vicinity of a diffuse ferroelectric phase transition, the temperature dependence of the dielectric permittivity, ϵ , was traditionally described by the well-known quadratic relation:⁵

$$\frac{1}{\epsilon(f, T)} = \frac{1}{\epsilon_m(f)} \left(1 + \frac{[T - T_m(f)]^2}{2\Delta^2} \right), \quad (1)$$

where f is the frequency, T the temperature, ϵ_m the magnitude of the dielectric peak, T_m the position of the peak, and Δ a broadening parameter. A power relation³⁵ has also been widely used for the description of the DPT:

$$\frac{1}{\epsilon(f, T)} = \frac{1}{\epsilon_m(f)} \left(1 + \frac{[T - T_m(f)]^\gamma}{2\Delta^2} \right), \quad (2)$$

where γ ($1 < \gamma < 2$) is a constant expressing the degree of relaxation. When $\gamma = 1$, expression (2) describes the Curie–Weiss behavior of the ferroelectrics, while for $\gamma = 2$, expres-

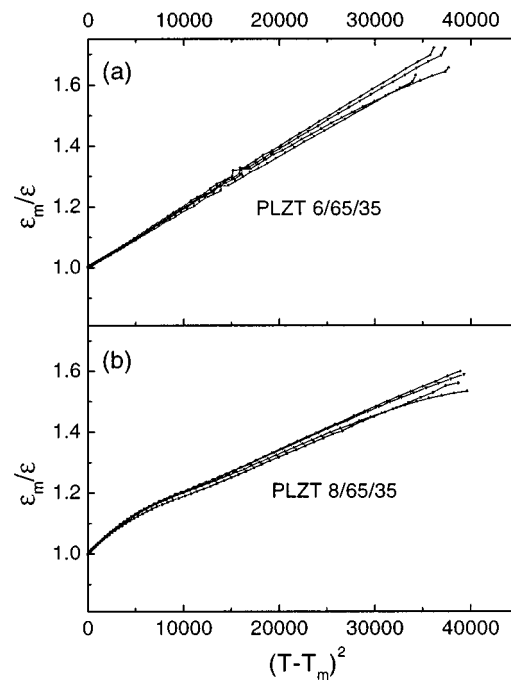


FIG. 11. ϵ_m/ϵ vs $(T - T_m)^2$ for (a) PLZT 6/65/35 and (b) PLZT 8/65/35 films with the grain size of 25 nm for different frequencies, where ϵ_m and T_m are the experimental magnitude and position, respectively, of the peak in the dielectric permittivity.

sion (2) is identical to Eq. (1). Although recent studies^{6–19} indicated that Eqs. (1) and/or (2) cannot characterize the experimental results adequately, we still used the expression (1) in our analysis. This allowed us to compare the properties of the produced films with the data obtained earlier for the bulk ceramic PLZT.³³

To determine the value of the parameter Δ for the peak, the ratio ϵ_m/ϵ was plotted vs $(T - T_m)^2$. The magnitude of the dielectric peak ϵ_m and the temperature T_m were extracted from the experimental data using the peak fitting procedure described in the previous chapter. Some of the curves are shown in Fig. 11. It can be seen that the dependence of ϵ_m/ϵ on $(T - T_m)^2$ was nearly linear. The slopes of the curves in Fig. 11 were slightly different for different temperature ranges and measurement frequencies. The values of parameter Δ were calculated using the expression

$$\Delta = \left[2 \left(\frac{\epsilon_m}{\epsilon} \right)' \right]^{-1/2}, \quad (3)$$

where $(\epsilon_m/\epsilon)'$ is the derivative obtained by differentiating the curves in Fig. 11. The results of the calculations are presented in Fig. 12.

The dependence of Δ on the temperature range and the measurement frequency was clearly seen in Fig. 12. In particular, a noticeable difference was found between the values of Δ in close proximity to the transition temperature and those about 50–100 °C away in PLZT 8/65/35 and PLZT 9.75/65/35 films.

The parameter Δ in PLZT 0/65/35 films was in the range 80–100 °C [Fig. 12(a)]. It is well known that a conventional ferroelectric transition occurs in bulk PLZT 0/65/35 on cooling. The broadening of the transition in PLZT 0/65/35 films,

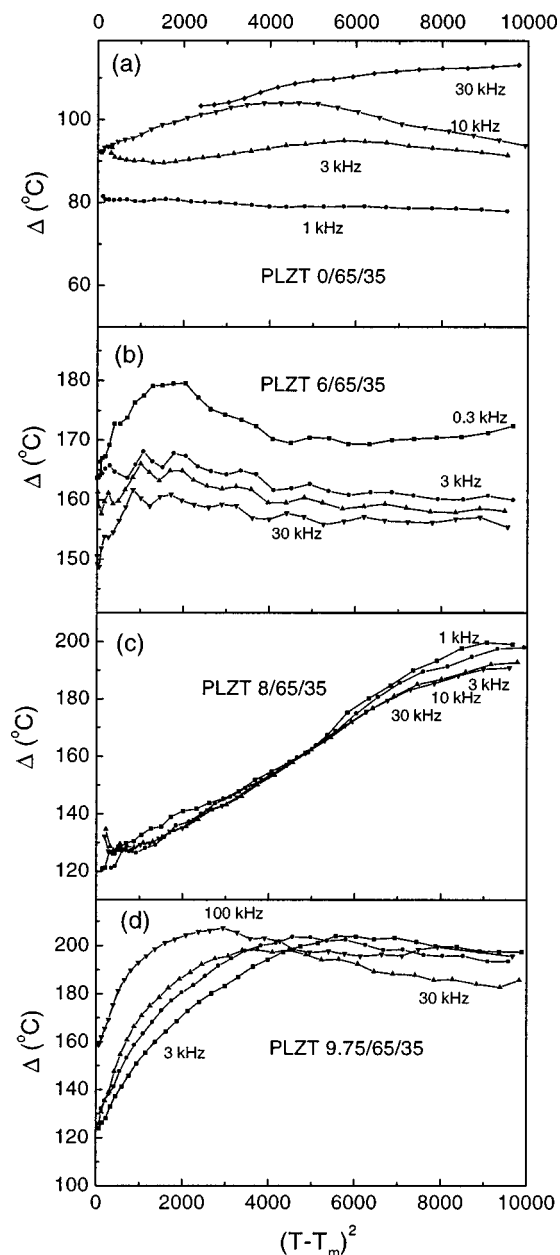


FIG. 12. Broadening parameter Δ as a function of frequency and temperature range for PLZT $x/65/35$ films of the first series with the grain size of about 25 nm: (a) $x=0$, (b) 6 at. %, (c) 8 at. %, (d) 9.75 at. %.

observed in the present work, was probably connected with the influence of the film interfaces. The modeling²⁵ accounting for the special conditions at the interfaces²⁵ has shown the possibility for the broadening of the peak around the bulk Curie point in the films. The parameter Δ , extracted formally from the results of the modeling,²⁵ could be of order $0.1-0.2T_m$. The value of Δ , found experimentally in PLZT 0/65/35 films, was in agreement with this range of values.

The film interfaces could also affect the values of Δ in the rest of the PLZT $x/65/35$ films. In fact, the observed broadening (Fig. 12) was typically in the range 100–200 °C, while the corresponding values of Δ in ceramic PLZT $x/65/35$ were around 30–100 °C. However, it was impossible to separate the contribution of the film interfaces and the contribution of the film material itself to the value of Δ .

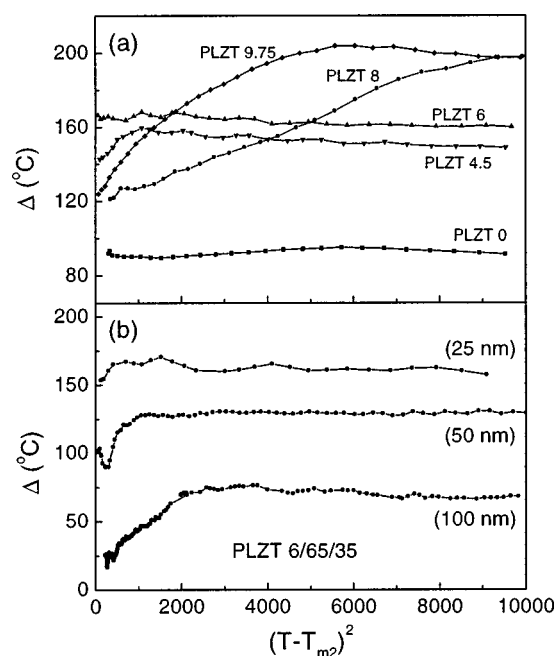


FIG. 13. Broadening parameter Δ determined at 1 kHz as a function of the La content in the films of the first series with (a) the grain size of 25 nm, and (b) as a function of the microstructure of PLZT 6/65/35 films (grain size is shown in brackets).

Only qualitative comparison of the transition broadening in PLZT films with that in PLZT ceramics could be performed.

From Fig. 13 it can be seen that the values of Δ depended both on the La content in the films and on their microstructure. Considering the temperature range in the close vicinity to the transition point, a nonmonotonic dependence of Δ on the La content could be found. The parameter Δ increased with increasing La content from 0 to 6 at. %, while the doping to 8–9.75 at. % led to a relative decrease of Δ . This nonmonotonic dependence was transformed into a monotonic increase of Δ with increasing La content at temperatures about 50–70 °C away from the transition point. The increase of Δ in PLZT 6/65/35 films, deposited under different conditions, correlated with the decrease in the grain size [Fig. 13(b)].

The dependence of the transition broadening, Δ , on the lanthanum content and on the microstructure of the films was in agreement with the behavior of the transition temperature (see the previous chapter). The same factors, which determined the temperature T_m , could also determine the broadening Δ . Such a possibility followed from the different model considerations, including e.g. the random field model¹⁵ and the models.^{36,37} The possible cause for the transition broadening in the reference³⁶ was attributed to the random distortions of the configurations of ions due to the existence of vacancies, dislocations and other defects. The smearing of the phase transition due to the influence of defects was shown in the analysis.³⁷ Despite the different methods used in the studies,^{15,36,37} the results obtained there indicated that the increase in the lanthanum content, the decrease of the grain size and the increase of the internal strain in the films could be responsible for the increase of the parameter

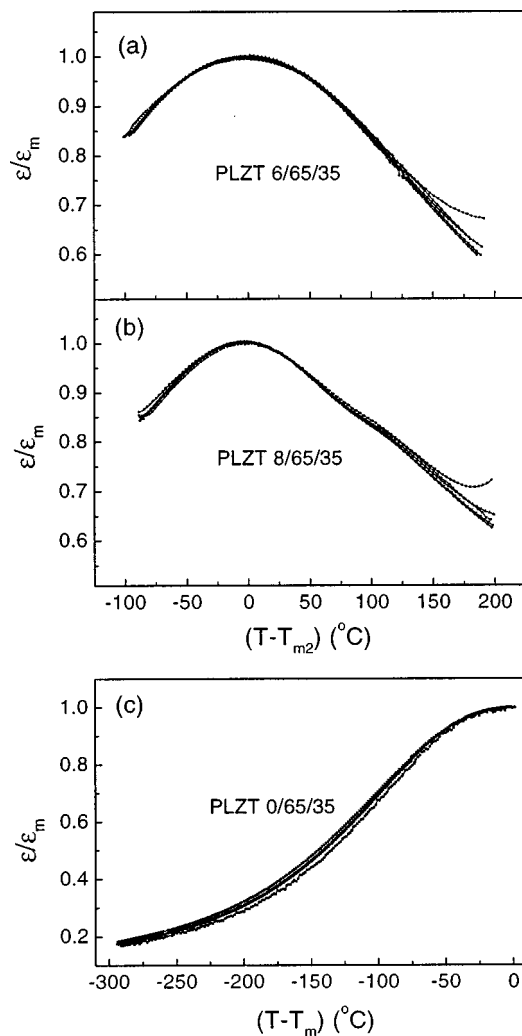


FIG. 14. Master curves, measured at different frequencies, for PLZT $x/65/35$ films: (a) $x=6$ at. %, (b) $x=8$ at. %, (c) $x=0$.

Δ . The experimental results in Figs. 12 and 13 were generally in agreement with these conclusions.

The analysis of the dielectric permittivity-temperature curves revealed that the value of Δ was dependent on the choice of the frequency and temperature ranges (Fig. 12). The phenomenon was experimentally observed and thoroughly studied in the ceramic $\text{PbMg}_{1/3}\text{Nb}_{2/3}\text{O}_3\text{--PbTiO}_3$ systems.^{13,19} Two sets of parameters were proposed for use in the description of $\epsilon(f, T)$:²⁰ one set related to the temperature dependence of the static dielectric permittivity and another to the temperature dependence of the relaxation time. The validity of the proposed description was confirmed in Ref. 20 by the existence of a master curve between the normalized dielectric permittivity, ϵ/ϵ_m , and the normalized temperature, $(T-T_m)$.

Master curves existed for the deposited PLZT films as well (Fig. 14). In contrast to Ref. 20, the master curves were obtained for the temperature ranges both above and below T_m . Another important peculiarity was that the master curves were obtained also for the PLZT 0/65/35 films. The observed characteristic features revealed that the dielectric peaks, measured at different frequencies in the films, origi-

nated, probably, from one mechanism. (The discussion about the mechanism remains open.^{2,8–20}) Moreover, in thin film heterostructures, the polarization relaxation processes can be considerably influenced by the film interfaces.

In conclusion to this chapter, the broadening, Δ , of the dielectric peak around T_m in PLZT $x/65/35$ films was found to be in the range of 80–200 °C. The larger than bulk values of Δ could be determined by the film interfaces. The value of Δ was a function of the La content in the film and the microstructure of the film. The broadening depended on the frequency and temperature ranges. Master curves between the normalized dielectric permittivity and the normalized temperature were obtained for PLZT films.

IV. CONCLUSIONS

Highly oriented stoichiometric perovskite PLZT $x/65/35$, $x=0\text{--}9.75$ at. %, films were formed by pulsed laser deposition onto LSCO/MgO substrates. The dielectric permittivity and loss tangent of the produced heterostructures were measured in the temperature range of 20–350 °C at frequencies of 100 Hz–1 MHz.

Peaks around 130–350 °C were observed in the dielectric permittivity (loss tangent)–temperature curves. The peaks exhibited a relaxor type behavior. The position of the peaks was a nonmonotonic function of the La content in the film and depended on the microstructure of the film.

The peak of the dielectric permittivity was broader than the corresponding peak in the bulk ceramic PLZT with the same composition, and the width depended on the composition and microstructure of the film. The broadening depended on the temperature and frequency ranges. Master curves between the normalized dielectric permittivity and normalized temperature were obtained for PLZT films.

The results were discussed in terms of the random field model for relaxor ferroelectrics and the models for finite size ferroelectrics.

ACKNOWLEDGMENTS

The authors wish to thank T. Murtoniemi for the assistance in the sample preparation and I. Shorubalko for the electrical characterization of the samples. The work was supported in part by the Department of Science and Education of Latvia and by the Academy of Finland. One of the authors (M.T.) acknowledges CIMO (Centre for International Mobility, Finland) for the financial support.

¹G. A. Smolenskii, V. A. Bokov, V. A. Isupov, N. N. Krainik, R. E. Pasynkov, and A. I. Sokolov, *Ferroelectrics and Related Materials* (Gordon and Breach, New York, 1984), p. 763.

²*Thin Film Ferroelectric Materials and Devices*, edited by R. Ramesh (Kluwer, Boston, 1997).

³See, e.g., overview Z. G. Ye, *Ferroelectrics* **184**, 193 (1996).

⁴G. Smolenskii and A. Agranovskaya, *Sov. Phys. Solid State* **1**, 1429 (1960).

⁵V. V. Kirillov and V. A. Isupov, *Ferroelectrics* **5**, 3 (1973).

⁶G. Burns and F. Dacol, *Phys. Rev. B* **28**, 2527 (1983).

⁷L. E. Cross, *Ferroelectrics* **76**, 241 (1987).

⁸S. Li, J. A. Eastman, R. E. Newnham, and L. E. Cross, *Phys. Rev. B* **55**, 12067 (1997).

⁹D. Viehland, J. F. Li, S. J. Jang, L. E. Cross, and M. Wuttig, *Phys. Rev. B* **43**, 8316 (1991).

- ¹⁰A. K. Tagantsev, Phys. Rev. Lett. **72**, 1100 (1994).
- ¹¹A. J. Bell, J. Phys.: Condens. Matter **5**, 8773 (1993).
- ¹²A. E. Glazounov, A. J. Bell, and A. K. Tagantsev, J. Phys.: Condens. Matter **7**, 4145 (1995).
- ¹³B. E. Vugmeister and H. Rabitz, Phys. Rev. B **57**, 7581 (1998).
- ¹⁴Z. Y. Cheng, R. S. Katiyar, X. Yao, and A. S. Bhalla, Phys. Rev. B **57**, 8166 (1998).
- ¹⁵M. D. Glinchuk and R. Farhi, J. Phys.: Condens. Matter **8**, 6985 (1996).
- ¹⁶M. D. Glinchuk, R. Farhi, and V. A. Stephanovich, J. Phys.: Condens. Matter **9**, 10237 (1997).
- ¹⁷R. Pattnaik and J. Toulouse, Phys. Rev. Lett. **79**, 4677 (1997).
- ¹⁸K. P. O'Brien, M. B. Weissman, D. Sheehy, and D. D. Viehland, Phys. Rev. B **56**, R11365 (1997).
- ¹⁹A. E. Glazounov, A. K. Tagantsev, and A. J. Bell, Phys. Rev. B **53**, 11281 (1996).
- ²⁰Z. Y. Cheng, P. S. Katiyar, X. Yao, and A. Guo, Phys. Rev. B **55**, 8165 (1997).
- ²¹See, e.g., *Ferroelectric Thin Films V*, edited by S. B. Desu, R. Ramesh, B. A. Tuttle, R. E. Jones, and I. K. Yoo [Mater. Res. Soc. Symp. Proc. **433** (1996)].
- ²²D. Schwenk, F. Fishman, and F. Schwabl, J. Phys.: Condens. Matter **2**, 5409 (1990).
- ²³W. L. Zhong, B. D. Qu, P. L. Zhang, and Y. G. Wang, Phys. Rev. B **50**, 12375 (1994).
- ²⁴Y. G. Wang, W. L. Zhong, and P. L. Zhang, Phys. Rev. B **51**, 5311 (1995).
- ²⁵B. Qu, W. Zhong, and P. Zhang, Phys. Rev. B **52**, 766 (1995).
- ²⁶J. S. Speck and W. Pompe, J. Appl. Phys. **76**, 466 (1994); J. S. Speck, A. Seifert, W. Pompe, and R. Ramesh, *ibid.* **76**, 477 (1994); A. E. Romanov, W. Pompe, and J. S. Speck, *ibid.* **79**, 4037 (1996); C. M. Foster, W. Pompe, A. C. Daykin, and J. S. Speck, *ibid.* **79**, 1405 (1996); S. K. Streiffert, C. B. Parker, A. E. Romanov, M. J. Lefevre, L. Zhao, J. S. Speck, W. Pompe, C. M. Foster, and G. R. Bai, *ibid.* **83**, 2742 (1998); A. E. Romanov, M. J. Lefevre, J. S. Speck, W. Pompe, S. K. Streiffert, and C. M. Foster, *ibid.* **83**, 2754 (1998).
- ²⁷J. Levoska, T. Murtoniemi, J. Lappalainen, and S. Leppävuori, Ferroelectrics **186**, 207 (1996).
- ²⁸M. Tyunina, J. Levoska, and S. Leppävuori, J. Appl. Phys. **83**, 5489 (1998).
- ²⁹M. H. Yeh, K. S. Liu, Y. C. Ling, J. P. Wang, and I. N. Lin, J. Appl. Phys. **77**, 5335 (1995); M. Okada and K. Tominaga, *ibid.* **71**, 1955 (1992); S. G. Ghonge, E. Roo, R. Ramesh, T. Sands, and V. G. Keramidas, Appl. Phys. Lett. **63**, 1628 (1993); K. L. Saenger, R. A. Roy, K. F. Etzold, and J. J. Cuomo, Mater. Res. Soc. Symp. Proc. **200**, 115 (1990); B. Jiang, V. Balu, T. S. Chen, S. H. Kuah, and J. C. Lee, *ibid.* **433**, 267 (1996); T. K. Song, S. Aggarwal, A. S. Prakash, B. Yang, and R. Ramesh, Appl. Phys. Lett. **71**, 2211 (1997); K. R. Udayakumar, P. J. Schuele, J. Chen, S. B. Krupanidhi, and L. E. Cross, J. Appl. Phys. **77**, 3981 (1995).
- ³⁰B. K. Chiang, L. P. Cook, P. K. Schenk, P. S. Brody, and J. M. Benedetto, Mater. Res. Soc. Symp. Proc. **200**, 133 (1990); J. Lee and R. Ramesh, Appl. Phys. Lett. **68**, 484 (1996); P. Tiwari, T. Zheleva, and J. Narayan, *ibid.* **63**, 30 (1993); M. Masuda, Y. Yamanaka, M. Tazoe, Y. Yonezawa, A. Morimoto, and T. Shimizu, Jpn. J. Appl. Phys., Part 1 **34**, 5154 (1995).
- ³¹Y. Yano, K. Iijima, Y. Daitoh, T. Terashima, Y. Bando, Y. Watanabe, H. Kasatani, and H. Terauchi, J. Appl. Phys. **76**, 7833 (1994).
- ³²N. A. Pertsev, A. G. Zembilgotov, and A. K. Tagantsev, Phys. Rev. Lett. **80**, 1988 (1998).
- ³³A. Sternberg, Doctoral thesis, University of Latvia, Riga, 1978.
- ³⁴K. Ishikawa, K. Yoshikawa, and N. Okada, Phys. Rev. B **37**, 5852 (1988), and references therein.
- ³⁵H. T. Martirena and J. C. Burfoot, Ferroelectrics **7**, 151 (1974).
- ³⁶A. A. Bokov, JETP **84**, 994 (1997).
- ³⁷A. P. Levanyuk, S. A. Minyukov, and M. Vallade, J. Phys.: Condens. Matter **9**, 5313 (1997).